Available online at www.sciencedirect.com
ScienceDirect
International Journal of Pharmaceutics 344 (2007) 103–109
INTERNATIONAL JOURNAL OF PHARMACEUTICS
www.elsevier.com/locate/ijpharm

Influence of surface charge and inner composition of porous nanoparticles to cross blood–brain barrier in vitro

Youssef Jallouli, Archibald Paillard, Jiang Chang, Emmanuel Sevin, Didier Betbeder*

Blood Brain Barrier Laboratory, EA 2465, IMPRT, IFR 114, Faculté des Sciences Jean Perrin, Université d'Artois, 62307 Lens, France

Received 15 February 2007; received in revised form 15 May 2007; accepted 6 June 2007
Available online 22 June 2007

Abstract

The aim of these studies was to evaluate the binding, uptake and transcytosis of 60 nm porous nanoparticles (NPs) that differed in their surface charge and inner composition on the blood–brain barrier (BBB). They were prepared from maltodextrins derived with or without a cationic ligand. In the cationic NPs an anionic lipid was inserted in their core to give DPPG-NPs. The data showed that at 4 °C the three NPs bind in different areas on endothelial cells: cationic NPs were found mainly around the paracellular area, while neutral NPs were mainly on the cell surface and DPPG-NPs binding was found at both paracellular areas and on the surface of the cells. At 37 °C neutral and cationic NPs had similar degrees of binding and uptake and were transcytosed. Filipin treatment increased their binding and uptake suggesting that sterols are implied in their efflux. Neutral NPs transcytosis was also inhibited by filipin. This inhibition shows that neutral NPs, like LDL in this model, use the caveolae pathway. Neutral and cationic 60 nm porous NPs are potential candidates for drug delivery to the brain.

Keywords: Nanoparticles; Blood–brain barrier; Binding and uptake; Transcytosis

1. Introduction

Drug delivery to the central nervous system (CNS) is one of the most challenging fields of research and development for pharmaceutical and biotechnology industries. Most of hydrophilic therapeutic agents, such as antibiotics, anticancer agents, and almost all newly developed neuropeptides do not cross the blood–brain barrier (BBB) after systemic administration (Pardridge, 2003). The blood–brain barrier (BBB) is composed of specific structures created by brain capillary endothelial cells and sheathing by astrocytic endfeet through the basement membrane, which maintains homeostasis of central nervous system by its specific properties. BBB differs from peripheral capillaries because it is influenced by surrounding neurons and astrocytes (Rubbin and Staddon, 1999). As a result brain capillary endothelial cells are characterized by narrow tight junctions, low pinocytic activity and high metabolic activity, little paracellular and no transcellular transport of high molecular compounds. Therefore research of CNS delivery of candidate drugs must be placed more emphasis on with BBB drug targeting technology. The use of nanocarriers, such as liposomes or polymeric nanoparticles may be advantageous over the current strategies (Tiwari and Amiji, 2006). These nanocarriers not only mask BBB limiting characteristics of therapeutic drugs molecule, but may also protect drugs from chemical/enzymatic degradation. Reduction of toxicity to peripheral organs can also be achieved with these nanocarriers. However when these nanoparticles are injected in the blood, they are quickly covered by opsonins which allows macrophages of the mononuclear phagocytic system (MPS) to easily recognize and remove these drug delivery devices before they can perform their designed therapeutic function. To avoid opsonisation nanoparticles can be covered by hydrophilic polymers such as PEG and specific ligands can be attached for brain targeting (Owens and Peppas, 2006).

Promising brain delivery results were obtained with polyalkylcyanoacrylate nanoparticles and it was shown that

Abbreviations: BBB, blood–brain barrier; BCECs, brain capillary endothelial cells; DiI, 1,1′-dioctadecyl-3,3,3′,3′-tetramethylindocarboxycyanate perchlorate; DMEM, Dulbecco's modified Eagle's medium; DPPG, dipalmitoyl phosphatidyl glycerol; FITC, fluorescein iso thiocyanate; NPs, nanoparticles; Pe, endothelial permeability coefficient; PBS-CMF, phosphate buffered saline calcium magnesium free; RH, Ringer–Hepes

* Corresponding author. Tel.: +33 3 21 79 17 08; fax: +33 3 21 79 17 36.
E-mail address: dbetbeder@aol.com (D. Betbeder).

0378-5173/$ – see front matter © 2007 Elsevier B.V. All rights reserved.
doi:10.1016/j.ijpharm.2007.06.023

these nanoparticules cross the BBB both in vitro and in vivo. Their ability to cross the BBB was linked to apolipoprotein binding of nanoparticles after i.v. administration and not to toxicity induced-tight junction aperture (Alyaudtin et al., 2001; Kreuter et al., 2002; Kim et al., 2007; Petri et al., 2007;). To investigate the mechanisms of BBB transport we developed an in vitro model that closely mimics in vivo conditions (Dehouck et al., 1990). It consists of a co-culture of brain endothelial cells co-cultured with astrocytes. In this model and other models made of brain capillary endothelial cells the transcytosis of natural nanoparticles, such as LDL, HDL and macromolecules such as transferring and lactoferrin, was found occurs through a caveolin-dependent pathway (Dehouck et al., 1997; Fenart et al., 2003; Balazs et al., 2004). To develop rational targeting strategies using NPs It is important to fully understand the binding and uptake mechanisms inducing their endocytosis and potential transcytosis. In a previous study we showed that NPs surface modification could strongly modify their transcytosis (Fenart et al., 1999).

In this study we evaluated the binding and uptake of neutral and cationic porous 60 nm NPs as potential drug carriers to cross the BBB. In particular the influence of the charge (cationic or neutral) and of the insertion of phospholipids in the core of cationic NPs was examined.

2. Materials and methods

2.1. Materials

Maltodextrin purchased from Roquette (France), [U-^{14}C]sucrose (677 mCi/mmol) was obtained from Amersham Laboratories (Les Ulis, France), 1,2-dipalmitoyl-*sn*-glycero-3-phosphatidylglycerol (DPPG) from lipoid (Germany), 5-([4,6-dichlorotriazin-2-yl]amino) fluorescein, 5-([4,6-dichlorotriazin-2-yl]amino) rhodamin, filipin, Albumin (bovine serum albumin) and 1,1′-dioctadecyl3,3,3′,3′-tetramethylindocarboxycyanate perchlorate (DiI) from Sigma Chemical Co. (Saint Louis, MO), 1-chloro-2,3-epoxypropan (epichlorhydrin) and glycidyltrimethylammonium chloride (hydroxycholine) from Fluka (Saint-Quentin-Fallavier, France). Nanosep 30K omega filters were obtained from Pall Corporation.

Bovine brain capillary endothelial cells (BCECs) were isolated and characterized as described by Meresse et al. (1989).

Rat astrocytes. Primary cultures of mixed astrocytes were obtained as described (Booher and Sensenbrenner, 1972).

2.2. Preparation, labeling and characterization of nanoparticles

Polysaccharide particles were prepared from US Pharmacopoeia maltodextrin as described previously (Major et al., 1997; Loiseau et al., 2002). Briefly, 100 g of maltodextrin was dissolved in 2 N sodium hydroxide with magnetic stirring at room temperature. Addition to the crude mixture of 1-chloro-2,3-epoxypropane (epichlorhydrin), or of a mixture of epichlorhydrin and glycidyltrimethylammonium chloride (hydroxycholine, cationic ligand) yielded neutral and cationic polysaccharide gels, respectively. The gels were then neutralised with acetic acid and sheared under high pressure in a Minilab homogenizer (Rannie; APV Baker, Evreux, France). The 60 nm neutral and cationic polysaccharide nanoparticles obtained were ultra-filtered on an SGI Hi-flow system (hollow fiber module: 30 UFIB/1 S.6/40 kDa; Setric Génie Industriel, Toulouse, France) to remove low-molecular weight reagents and salts.

Covalent labeling of the polysaccharidic core with fluorescein or rhodamin was achieved by covalently binding either fluorescein isothiocyanate or rhodamin isothiocyanate to the polysaccharidic core (Prieur et al., 1996). These labeled particles were washed and purified by ultrafiltration on an SGI Hi-flow system (30UFIB/1S.6/40 kDa) with 1 M NaCl and with demineralized water until no free marker was detected in the ultra-filtrate. The labeled polysaccharidic particles (1 mg/ml) were stored in sterile tubes after filtration through a 0.2 μm filter. Due to poor fluorescence stability rhodamin labeling was used for neutral NPs for fluorescence imaging only. Fluorescein labeled NPs were used for quantitative analysis. The binding of fluorescein to the NPs was covalent and no release was observed at 37 °C after 4 h incubation in cellular medium.

Cationic nanoparticles in which anionic phospholipids were incorporated in their core (DPPG-NPs), were prepared by mixing polysaccharide nanoparticles (Loiseau et al., 2002), DPPG and DiI at a temperature above the gel-to-liquid phase transition temperature of the phospholipid (Woodle and Papahadjopoulos, 1989). Polysaccharide and phospholipid concentrations were 10 and 7 mg/ml, respectively. The mean diameter of NPs was determined by laser light scattering with the N4 MD Coulter nanoparticle analyzer (Coultronics, Margency, France). The zeta-potential of nanoparticles were determined by photon correlation spectroscopy (ZetaSizer II, Malvern Instruments) in 15 mM NaCl.

2.3. Cell culture

2.3.1. Preparation of filters for coculture

Culture plate inserts (Millicell PC 3 μm, 30 mm diameter; Millipore, SAS, Molsheim, France) were coated on the upper side with 150 μl of a 2 mg/ml solution of rat tail collagen containing 10-fold concentrated DMEM plus 0.3 M NaOH. The coated inserts were dried for 1 h at 37 °C and were rinsed twice with water and once with PBS-CMF before being placed in complete medium.

2.3.2. Brain capillaries endothelial cells

The cell culture was performed according to (Dehouck et al., 1992), briefly bovine BCECs were isolated and characterized as described by Meresse et al. (1989). The endothelial cells were cultured in the presence of DMEM supplemented with 10% (v/v) heat inactivated calf serum and 10% (v/v) horse serum (Invitrogen), 2 mM glutamine, 50 μg/ml gentamicin, and basic fibroblast growth factor (1 ng/ml, added every other day).

2.3.3. Coculture of BCECs and glial cells

Primary cultures of mixed glial cells composed of 60% astrocytes, 20% oligodendrocytes, and 20% microglia were pre-

pared from newborn rat cerebral cortex. After removing the meninges, the brain tissue was forced gently through a nylon sieve, as described by Booher and Sensenbrenner (1972). Glial cells were plated on six multiwell dishes at a concentration of 1.2×10^5 cells/ml in 2 ml of DMEM supplemented with 10% (v/v) fetal calf serum (Invitrogen), and the medium was changed twice a week. Three weeks after seeding, cultures of glial cells were stabilized and used for coculture. Coated filters were set in six multiwell dishes containing glial cells. Endothelial cells were plated on their upper side in 1.5 ml of medium at a concentration of 4×10^5 cells/ml. The coculture medium was the same as that for BCECs. Under these conditions, BCECs formed a confluent monolayer after 7 days. Experiments were performed 5 days after confluence.

2.4. Evaluation of the ability of the nanoparticles to cross collagen-coated filters

The experiments were performed at 37 °C in humified atmosphere with 5% CO_2. The coated inserts were rinsed twice with RH solution and were transferred into six-well plate containing RH solution (2,5 ml in abluminal side). RH solution (1.5 ml) containing 120 μg of NPs labeled with FITC, rhodamine or DiI was placed, at time 0, in the upper compartment (luminal side). At different interval times, inserts were transferred to other wells to minimize the possibility of passage from the lower compartment. For each condition, three inserts without cells were assayed. The quantity of nanoparticles was determined by quantitative fluorescence analysis.

2.5. Binding studies at 4 °C

Prior to binding studies, the luminal and abluminal side of the coculture were washed twice with cold RH solution. Once filters containing endothelial cells were transferred into six-well plate containing RH solution (2.5 ml in abluminal side), RH solution (1.5 ml) containing 120 μg of NPs was placed, at time 0, in the upper compartment (luminal side). The incubations were performed at 4 °C. After 45 min, the cells were washed twice with RH solution followed with twice washing with BSA 2% solution and finally with RH solution twice time at 4 °C. BCECs were fixed with 4% paraformaldehyde in PBS-CMF at room temperature. The filters and their attached monolayers were mounted on glass microscope slides with Mowiol mountant (Hoechst, Frankfurt, Germany), and the specimens were visualized and photographed with fluorescence microscope (Leica, Wetzlar, Germany).

2.6. Binding, uptake and transcytosis of NPs

The binding, uptake and transcytosis experiments were performed at 37 °C in RH buffer. At different intervals times: 120, 180 and 240 min, inserts were transferred to other wells. For each condition, three inserts with BCECs monolayer were assayed. Amounts of NPs fixed and internalized by the endothelial cells were indirectly evaluated by quantitative analysis of fluorescence in the upper compartment. Nanoparticle integrity in the lower compartment was checked using nanosep filtration. The transcytosis studies were evaluated by quantification of fluorescence in lower compartment. These analysis were performed using a Fluoroskan. Fluorescein or DiI fluorescence excitation and emission spectra wavelengths λ_{ex} and λ_{em} was 485 and 538 nm or 540 and 584 nm, respectively. For each test compound, quantification was obtained from a standard curve. Experiments were performed in triplicate and the data are represented as means ± S.E.

2.7. Integrity of the BCECs monolayer

Using the same procedure, the integrity of BCECs monolayers was checked by adding [^{14}C] sucrose in the upper compartment containing the different test nanoparticles. Amounts of radiotracers in the lower compartment were measured in a liquid scintillation counter (Wallac 14110; Pharmacia, Piscataway, NJ). The endothelial permeability coefficient (Pe in cm/min) was calculated as previously described (Dehouck et al., 1992). Only experiment values where Pe of sucrose was$< 1 \times 10^{-3}$ cm/min was taken into account.

2.8. Treatment with filipin

The BCECs monolayers were pretreated or not with 10 μg/ml of filipin for 15 min at 37 °C in humified atmosphere with 5% CO2. They were washed with RH and 120 μg of nanoparticles was added to the cells and the transport studies analysed as described above. As control transferrin-FITC transcytosis was evaluated in presence or not of filipin in order to check the cellular differentiation (Boveri et al., 2005).

2.9. Statistical analysis

The means and standard errors for all values were calculated. For simple comparisons a one-way analysis of variance (ANOVA). The difference was considered as significant when $P < 0.05$.

3. Results

3.1. Characterization of nanoparticles

Three types of porous NPs constructed from a maltodextrin backbone were prepared. The average size and polydispersity of these NPs was similar (Table 1). There were no differences in

Table 1
Particle size and zeta potential of NPs ($n = 3$)

Nanoparticles	Mean size (mean ± S.D., nm)	p.i.	Zeta potential (mV)
Cationics NPs	60 ± 13.1	0.21	+25 ± 1.5
Cationics DPPPG-NPs	61 ± 12.3	0.25	+24 ± 1.1
Neutrals NPs	59 ± 22.7	0.28	0 ± 1

Zeta potential was measured in NaCl solution (15 mM). p.i.: polydispersity index.

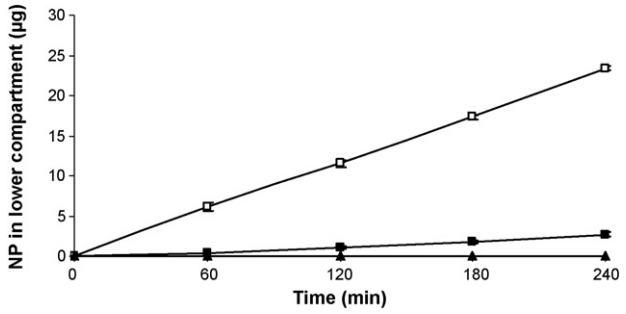

Fig. 1. Evaluation of the ability of NPs to cross collagen-coated filters. Neutral NPs (square and open symbols), cationic NPs (square and closed symbols) or DPPG-NPs (triangular closed symbols). Each point was performed in triplicate and the data are represented as means ± S.E. ($n = 3$).

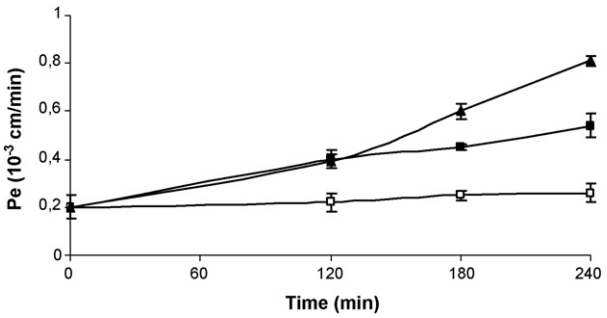

Fig. 2. BBB permeability studies of ^{14}C-labelled sucrose in vitro in the presence of neutral NPs (square open symbols), cationic NPs (square closed symbols) or DPPG-NPs (triangular closed symbols); $n = 3$. The mean scores were statistically significant when evaluated using one-way ANOVA ($p < 0.001$). *$p < 0.05$, **$p < 0.01$ vs. control ($n = 3$ BCECs monolayers/treatment; Dunnet test).

particle size and zeta potential between cationic NPs and cationic DPPG-NPs which suggest that DPPG incorporates into the core of cationic NPs. The porosity of these NPs allows the insertion of macromolecules within the core without modifying their surface before reaching saturation. DPPG-NPs can be used as reservoir for lipophilic drugs (Loiseau et al., 2002).These colloids are highly hydrophilic and very stable in solution in terms of size and chemical composition (>12 months).

3.2. Ability of NPs to cross collagen-coated filters

In order to evaluate the transcytosis of the NPs we tested whether they can cross collagen-coated filters without cells. Fig. 1 shows that neutral nanoparticles diffuse from the upper to the lower compartment faster than cationic NPs, suggesting that neutral NPs have a lower affinity to collagen-coated filters. DPPG-NPs do not diffuse through the collagen-coated filters. These results show that the ability of the NPs to cross collagen-coated filters is dependent on the surface charge and inner composition of each type of nanoparticles.

3.3. Integrity of the BCECs monolayer in the presence of NPs

The integrity of BCECs endothelial cells was evaluated using ^{14}C-labelled sucrose as a paracellular marker. The Pe of sucrose, in the presence of neutral, cationic or DPPG-NPs, was$< 1 \times 10^{-3}$ cm/min, for each experimental conditions (Fig. 2). These results show that the integrity of the BBB was preserved during the experiments. In these studies only experiments where the sucrose Pe was$< 1 \times 10^{-3}$ cm/min were taken into account.

3.4. Binding of NPs to BCECs

The binding of NPs to endothelial cells was evaluated at 4 °C using fluorescence microscopy (Fig. 3). Neutral NPs were mainly observed on the cell surface (Fig. 3A), while cationic NPs were mainly found in the paracellular area (Fig. 3B). DPPG-NPs had an intermediate behavior as they associated with both the surface and the paracellular area of endothelial cells (Fig. 3C). These results suggest that inner composition and surface charge of these porous NPs play a key role in their binding.

3.5. Binding and uptake of NPs

Binding and uptake was evaluated from 120 min to 240 min at 37 °C using quantitative fluorescence (Fig. 4). We observed that the kinetics of binding and uptake of cationic and neutral NPs slightly decreased, while DPPG-NPs binding and uptake increased (Fig. 4). The decrease of binding and uptake of cationic and neutral NPs could be explained by their efflux to the luminal side (Zhang et al., 2006). To elucidate whether the uptake was caveolae-dependent we treated the cells with filipin, a sterol-binding agent, known to interfere with the caveolae-dependent pathway (Schnitzer et al., 1994). The increase in the binding and uptake of neutral and cationic NPs observed could suggest that their efflux is sterol-dependent (Fig. 5).

3.6. Evaluation of transcytosis of neutral and cationic NPs

To investigate if NPs cross the BBB the experiments were performed at 37 °C on cells adsorbed on collagen-coated filters. The kinetics of arrival of NPs in the abluminal chamber were analysed. Due to high collagen binding of DPPG-NPs only neutral and cationic NPs were evaluated. Fig. 6 shows the transcytosis of the NPs in presence or absence of filipin (Schnitzer et al., 1994). Nanosep filtration of the transcytosed NPs confirmed that they were not degradated. Neutral and cationic NPs cross the BBB using transcytosis as no paracellular aperture was observed (Fig. 2). Transcytosis of the neutral NPs (Fig. 6A) was higher than cationic NPs (Fig. 6B). Filipin inhibits neutral NPs transcytosis (Fig. 6A) but not cationic NPs (Fig. 6B). As a control, we verified that the transcytosis of transferrin was inhibited by filipin (Fenart and Cecchelli, 2003).

4. Discussion

To evaluate transport through the BBB we developed an in vitro model based on a coculture of brain endothelial and glial cells. This coculture retains all endothelial cell markers and the

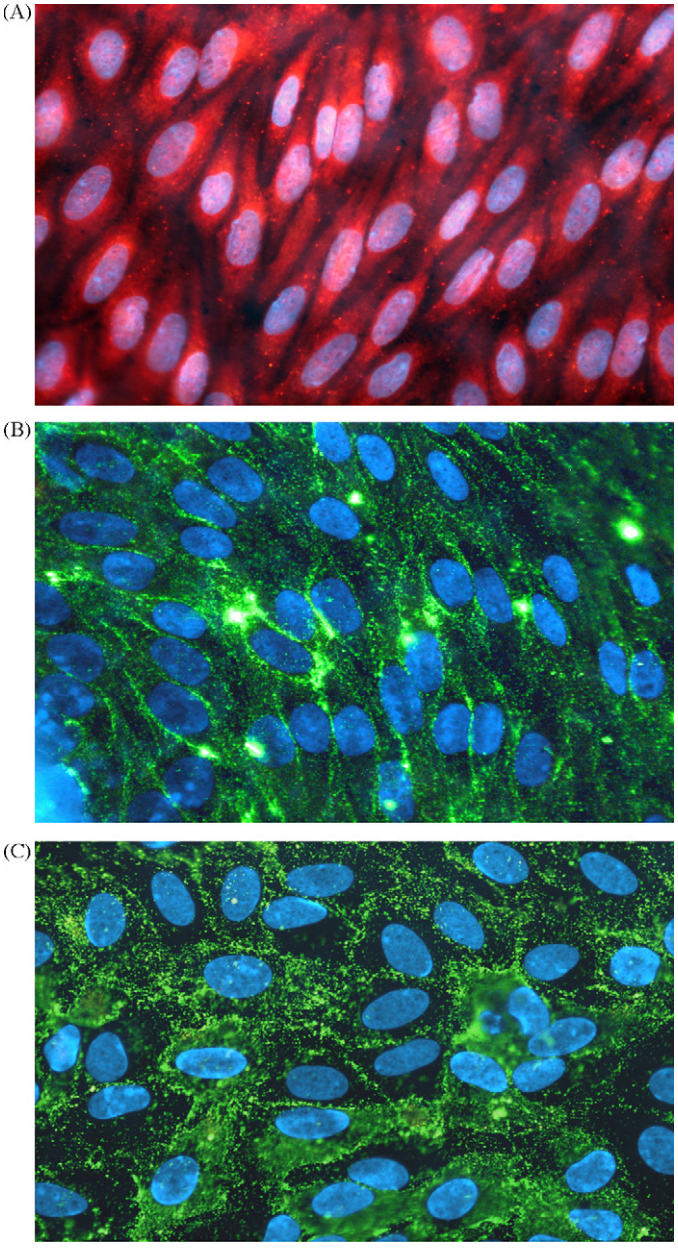

Fig. 3. Evaluation of NPs binding on BBB at 4 °C using fluorescence microscopy. Neutral NPs were labelled with rhodamine (A), and cationic NPs (B) and DPPG-NPs (C) were labelled with FITC. The nucleus were labelled with Hoechst.

characteristics of the blood–brain barrier, including tight junctions and gamma-glutamyl transpeptidase activity (Dehouck et al., 1990). A good *in vitro–in vivo* correlation of a set of compounds having a wide range of lipid solubility was obtained suggesting that this model is relevant (Dehouck et al., 1992). The coculture of BCECs and glial cells induced low sucrose Pe and reflected the high degree of differentiation of the co-cultured cells (Boveri et al., 2005). One of the major problems of in vitro model studies is the loss of tight junction properties and differentiation due to cellular culture conditions or potential toxicities of the compounds tested. This tight junction rupture can happen within minutes after incubation with compounds and this was the reason why we followed the paracellular pathways of every co-

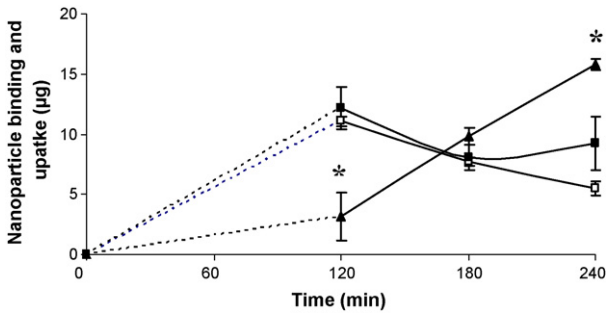

Fig. 4. Kinetics of binding and uptake of neutral NPs (square open symbols), cationic NPs (square closed symbols) or DPPG-NPs (triangular closed symbols) at 37 °C. The mean scores were statistically significant when evaluated using one-way ANOVA ($p < 0.001$). *$p < 0.05$, **$p < 0.01$ vs. control ($n = 3$ BCECs monolayers/treatment; Dunnet test).

culture during our studies using sucrose as a paracellular marker (Fig. 2).

Transcytosis of nanoparticles through the blood–brain barrier is a challenge for developing new drug delivery systems to target the brain. The results of the studies presented herein demonstrate that binding, uptake and transcytosis of 60 nm porous

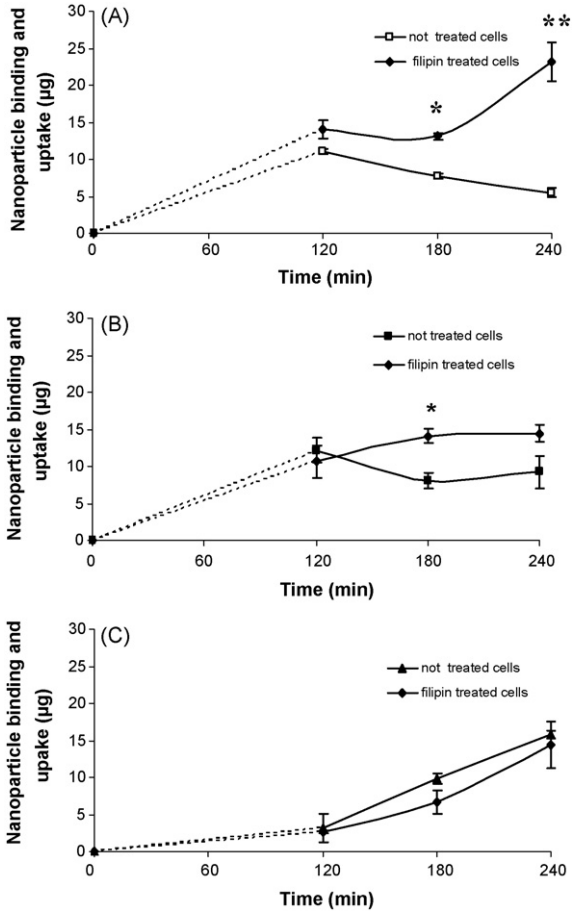

Fig. 5. Filipin's effect on the kinetics of binding and uptake of neutral NPs (Fig. 6A), cationic NPs (Fig. 6B) or DPPG-NPs (Fig. 6C) by BBB at 37 °C ($n = 3$) The mean scores were statistically significant when evaluated using one-way ANOVA ($p < 0.001$). *$p < 0.05$, **$p < 0.01$ vs. control ($n = 3$ BCECs monolayers/treatment; Dunnet test).

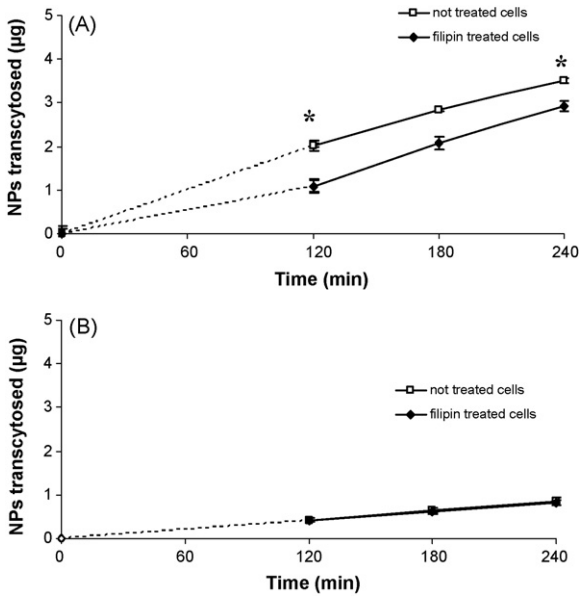

Fig. 6. Transport of 60 nm porous nanoparticles across BCECs monolayer. Untreated or BCECs pretreated or not with 10 μg/ml filipin were incubated with neutral NPs (A) or cationic NPs (B) at 37 °C for different times, respectively; $n = 3$. The mean scores were significant using one-way ANOVA ($p < 0.001$). *$p < 0.05$, **$p < 0.01$ vs. control ($n = 3$ BCEC monolayers/treatment; Dunnet test).

nanoparticles is dependent on their charge and inner composition. Neutral nanoparticles cross the cells using the caveolae pathway which is used by natural nanoparticles such as LDL and HDL in porcine and bovine models of BBB (Dehouck et al., 1997; Balazs et al., 2004). We also observed that the binding at 4 °C of these nanoparticles was homogenous on the surface of cells (Fig. 3A). The mechanisms allowing these particles to use the caveolae pathway is not understood. As these NPs are made of glucose we propose that glucose could allow their targeting to the brain as was observed in vivo for niosomes (Dufes et al., 2004). Glucose NPs are theoretically good candidates for targeting the brain. Indeed, glucose is the main source of energy in the brain and corresponds to almost 30% of the total glucose consumption in the body (Dick et al., 1984). This suggests that the glucose transportor (GLUT-1) might be an efficient target for the binding of NPs to the luminal side of endothelial cells (Cornford and Hyman, 2005). Then particles are endocytosed and taken through the caveolae pathway by an unknown mechanism (adsorptive endocytosis?). There is also a wide variety of membrane bound lectins that recognize sugars present on different glycoconjugates. These lectins might also be implicated in the adsorption and endocytosis of neutral NPs (Banks and Kastin, 1989; Weigel and Yik, 2002). Filipin increased the binding and uptake of neutral NPs suggesting that cholesterol rich rafts are implicated in their efflux. Further studies are necessary to fully understand the mechanisms implied.

Cationic NPs were found to bind at 4 °C to the paracellular area (Fig. 3A), which is an area that might be rich in anionic sites (Nagy et al., 1983). Anionic sites located on the luminal surface of the plasmalemma of the ECs mainly exist due to sialic acid residues of acidic glycoproteins (Vorbrodt, 1989). The binding of these nanoparticles is partially followed by their transcytosis via a process independent of the sterol-dependent pathway (Fig. 6B). Finally the insertion of DPPG in the core of cationic nanoparticles dramatically changed their behaviour in terms of collagen and cellular binding and uptake (Table 1, Figs. 1 and 4). These particles contrary to cationic NPs were also found not to activate complement activation (manuscript under preparation) and these results clearly show that the lipids inside their cores modify the properties of these porous NPs. However their strong affinity for collagen may limit the use of these particles in targeting the brain endothelial cell basement membrane from where drugs could diffuse to the brain.

5. Conclusion

We evaluated three porous NPs having the same internal backbone and size but differing by their surface an/or inner composition to cross BBB. We observed that even small modifications of these NPs such as inner composition dramatically change their behaviour in the presence of brain endothelial cells. DPPG-NPs transcytosis could not be evaluated due to high binding to collagen-coated filters. Neutral and cationic NPs are transcytosed and are potential candidates to deliver drugs to the brain.

Acknowledgements

We wish to thank Ceva santé animale and la region du Nord-Pas de Calais for financial support. We also wish to thank Pr R. Cecchelli and all the members of the laboratory for their help during the cell culture and for scientific advice, in particular Pr L. Fenart and Pr M.P. Dehouck.

References

Alyaudtin, R.N., Reichel, A., Lobenberg, R., Ramge, P., Kreuter, J., Begley, D.J., 2001. Interaction of poly(butylcyanoacrylate) nanoparticles with the blood–brain barrier in vivo and in vitro. J. Drug Target 9, 209–221.

Balazs, Z., Panzenboeck, U., Hammer, A., Sovic, A., Quehenberger, O., Malle, E., Sattler, W., 2004. Uptake an transport oh high-density lipoprotein (HDL) and HDL associated alpha-tocopherol by an in vitro blood–brain barrier model. J. Neurochem. 89, 939–950.

Banks, W.A., Kastin, A.J., 1989. Characterization of lectin-mediated brain uptake of HIV-1 GP120. J. Neurosci. Res. 54, 522–529.

Booher, J., Sensenbrenner, M., 1972. Growth and cultivation of dissociated neurons and glial cells from embryonic chick, rat and human brain in flask cultures. Neurobiology 2, 97–105.

Boveri, M., Berezowski, V., Price, A., Slupek, S., Lenfant, A.M., Benaud, C., Hartung, T., Cecchelli, R., Prieto, P., Dehouck, M.P., 2005. Induction of blood–brain barrier properties in cultured brain capillary endothelial cells: comparison between primary glial cells and C6 cell line. Glia 51, 187–198.

Cornford, E.M., Hyman, S., 2005. Localization of brain endothelial luminal and abluminal transporters with immunogold electron microscopy. NeuroRx 2, 27–43.

Dehouck, M.P., Jolliet-Riant, P., Bree, F., Fruchart, J.C., Cecchelli, R., Tillement, J.P., 1992. Drug transfer across the blood–brain barrier: correlation between in vitro and in vivo models. J. Neurochem. 58, 1790–1797.

Dehouck, M.P., Meresse, S., Delorme, P., Fruchart, J.C., Cecchelli, R., 1990. An easier, reproducible, and mass-production method to study the blood–brain barrier in vitro. J. Neurochem. 54, 1798–1801.

Dehouck, B., Fenart, L., Dehouck, M.P., Pierce, A., Torpier, G., Cecchelli, R., 1997. A new function for the LDL receptor: transcytosis of LDL across the blood–brain barrier. J. Cell Biol. 138, 877–889.

Dick, A.P., Harik, S.I., Klip, A., Walker, D.M., 1984. Identification and characterization of the glucose transporter of the blood–brain barrier by cytochalasin B binding and immunological reactivity. Proc. Natl. Acad. Sci. U.S.A. 81, 7233–7237.

Dufes, C., Gaillard, F., Uchegbu, I.F., Schatzlein, A.G., Olivier, J.C., Muller, J.M., 2004. Glucose-targeted niosomes deliver vasoactive intestinal peptide (VIP) to the brain. Int. J. Pharm. 285, 77–85.

Fenart, L., Casanova, A., Dehouck, B., Duhem, C., Slupek, S., Cecchelli, R., Betbeder, D., 1999. Evaluation of effect of charge and lipid coating on ability of 60-nm nanoparticles to cross an in vitro model of the blood–brain barrier. J. Pharmacol. Exp. Ther. 291, 1017–1022.

Fenart, L., Cecchelli, R., 2003. Protein transport in cerebral endotheliumIn vitro transcytosis of transferrin. Methods Mol. Med. 89, 277–290.

Kim, H.R., Gil, S., Andrieux, K., Nicolas, V., Appel, V., Chacun, H., Desmaele, D., Taran, F., Georgin, D., Couvreur, P., 2007. Low-density lipoprotein receptor-mediated endocytosis of Pegylated nanoparticles in rat brain endothelial cells. Cell. Mol. Life Sci. (Epub ahead of print).

Kreuter, J., Shamenkov, D., Petrov, V., Ramge, P., Cychutek, K., Koch-Brandt, C., Alyautdin, R., 2002. Apolipoprotein-mediated transport of nanoparticle-bound drugs across the blood–brain barrier. J. Drug Target 10, 317–325.

Loiseau, P.M., Imbertie, L., Bories, C., Betbeder, D., De Miguel, I., 2002. Design and antileishmanial activity of amphotericin B-loaded stable ionic amphiphile biovector formulations. Antimicrob. Agents Chemother. 46, 1597–1601.

Major, M., Prieur, E., Tocanne, J.F., Betbeder, D., Sautereau, A.M., 1997. Characterization and phase behaviour of phospholipid bilayers adsorbed on spherical polysaccharidic nanoparticles. Biochim. Biophys. Acta 1327, 32–40.

Meresse, S., Dehouck, M.P., Delorme, P., Bensaid, M., Tauber, J.P., Delbart, C., Fruchart, J.C., Cecchelli, R., 1989. Bovine brain endothelial cells express tight junctions and monoamine oxidase activity in long-term culture. J. Neurochem. 53, 1363–1371.

Nagy, Z., Peters, H., Huttner, I., 1983. Charge-related alterations of the cerebral endothelium. Lab. Invest. 49, 662–671.

Owens 3rd., D.E., Peppas, N.A., 2006. Opsonization, biodistribution, and pharmacokinetics of polymeric nanoparticles. Int. J. Pharm. 307, 93–102.

Pardridge, W.M., 2003. Blood–brain barrier drug targeting: the future of brain drug development. Mol. Interv. 3, 90–105.

Petri, B., Bootz, A., Khalansky, A., Hekmatara, T., Muller, R., Uhl, R., Kreuter, J., Gelperina, S., 2007. Chemotherapy of brain tumout using doxorubicin bound to surfactant-coated poly(butylcyanoacrylate) nanoparticles: revisting the role of surfactants. Contr. Rel. 117, 51–58.

Prieur, E., Betbede, r, D., Niedergang, F., Major, M., Alcover, A., Davignon, J.L., Davrinche, C., 1996. Combination of human cytomegalovirus recombinant immediate-early protein (IE1) with 80 nm cationic biovectors: protection from proteolysis and potentiation of presentation to $CD4^+$ T-cell clones in vitro. Vaccine 14, 511–520.

Rubbin, L.L., Staddon, J.M., 1999. The cell biology of the blood–brain barrier. Annu. Rev. Neurosci. 22, 11–28 (Review).

Schnitzer, J.E., Oh, P., Pinney, E., Allard, J., 1994. Filipin-sensitive caveolae-mediated transport in endothelium: reduced transcytosis, scavenger endocytosis, and capillary permeability of select macromolecules. J. Cell Biol. 127, 1217–1232.

Tiwari, S.B., Amiji, M.M., 2006. A review of nanocarrier-based CNS delivery systems. Curr. Drug Deliv. 3, 219–232.

Vorbrodt, A.W., 1989. Ultracytochemical characterization of anionic sites in the wall of brain capillaries. Neurocytology 18, 359–368.

Weigel, P.H., Yik, J.H., 2002. Glycans as endocytosis signals: the cases of the asialoglycoprotein and hyaluronan/chondroitin sulfate receptors. Biochim. Biophys. Acta 1572, 341–363.

Woodle, M.C., Papahadjopoulos, D., 1989. Liposome preparation and size characterization. Methods Enzymol. 171, 193–217.

Zhang, Y., Hu, Z., Ye, M., Pan, Y., Chen, J., Luo, Y., Zhang, Y., He, L., Wang, J., 2006. Effect of poly(ethylene glycol)-block-polylactide nanoparticles on hepatic cells of mouse: low cytotoxicity, but efflux of the nanoparticles by ATP-binding cassette transporters. Eur. J. Pharm. Biopharm. 15 (ahead of print).